Statistical Analysis and Performance Evaluation for On-Body Radio Propagation With Microstrip Patch Antennas

Akram Alomainy, Yang Hao, Abdus Owadally, Clive G. Parini, Yuri Nechayev, Costas C. Constantinou, and Peter S. Hall

Abstract—On-body propagation channel measurements using two microstrip patch antennas for various links are presented and statistically analyzed. The attenuation attributed to factors such as the body, head and clothing are: 19.2, 13.0, and 1.7 dB, respectively, when measurement performed in the anechoic chamber. Measured cumulative distribution function (CDF) of data in the chamber and lab fits to lognormal distribution with deviation factors comparable in both cases. The results demonstrate that the human body is a major shadowing contributor in body area network (BAN) radio systems. The performance of potential radio systems under the measured channel variations is also investigated. Excellent system performance is achievable with power levels as low as 0.01 mW. These results support the significance of channel characterization and modelling in producing suitable wireless systems for ultra low power BANs.

Index Terms—Bit error rate (BER), body area network, microstrip antenna, on-body propagation.

I. INTRODUCTION

Wireless body-centric networks (WBAN) have recently received an increasing attention due to their promising applications in medical sensor systems and personal entertainment technologies [1]–[4]. Major drawback of current body worn systems is the wired communication which is often undesirable because of the inconvenience for the user. Other connection methods have been proposed for solving this problem, including the use of smart textiles and communication by the currents on the user's body [5]. Smart clothes imply the need for a special garment to be worn, which may conflict with the user's personal preferences. Similarly, the body current communication is limited because it has a relatively low capacity and not suitable for very high data rate applications. Wireless body-centric network presents the apparent option and is aiming to provide systems with constant availability, re-configurability, unobtrusiveness and true extension of a human's mind.

The wireless body-centric network has a rapidly changing radio links directly influencing the propagation channel characteristics and hence system performance. Radio channel characterization for on-body communication has been presented in few literatures [6]–[12], however, to the authors' knowledge, statistical analysis of extensive on-body channel measurement with channel models based on detailed experimental investigations and the effect of the measured channel variation on the system performance has not been presented, specifically for

TABLE I
MICROSTRIP PATCH ANTENNA PARAMETERS WHEN PLACED IN FREE SPACE AND ON THE BODY

Parameter		Free Space	On-Body
Resonance	Sim	2.41 GHz	2.42 GHz
	Meas	2.45 GHz	2.46 GHz
Bandwidth	Sim	30.1 MHz	35.0 MHz
	Meas	32.5 MHz	33.5 MHz
Gain	Sim	6.5 dB	5.8 dB
	Meas	6.7 dB	6.1 dB
Radiation efficiency	Sim	87%	75%
3dB Beamwidth	Sim	83^0	75^0
	Meas	76^0	72^0

propagation at 2.45 GHz. In this paper, on-body propagation channel measurements using two microstrip patch antennas for various links and different node positions are presented and statistically analyzed. Statistical channel models and parameters are applied in evaluating the performance of a simple radio system based on Bluetooth specifications utilizing Gaussian frequency shift keying (GFSK) transmission [16], [17]. The analysis provides a picture of the system behavior in such a dynamic environment, i.e. on-body communication, with various data rate and transmitted power levels.

The rest of the paper is organized as follows. Section II presents the on-body propagation measurement setup and the antenna used for radio channel characterization. On-body channel statistical models and parameters are derived and analyzed with respect to chamber and lab measurements and also with regards to various body positions and antenna placements. Section III investigates the performance of potential radio system including channel parameters obtained from previous section in order to study BER variations with different on-body links and also body movements. Section IV draws the main conclusions of the study presented here.

II. ON-BODY PROPAGATION CHANNEL CHARACTERIZATION

A. Measurement Setup

Propagation path loss of an on-body channel was measured using a vector network analyzer (VNA) and a pair of microstrip patch antennas following the procedure and antenna positions highlighted and detailed in [6]–[9], [11]. For each antenna placement set-up, the S21 response was measured every second while the person wearing the antennas (in an anechoic chamber and lab environment) assumed various body positions changing at every 20 s. The positions of the antennas on the body are shown in [6], [9]. Positions chosen for the measurement includes right side of the chest, left side of the back, right and left sides of the head and right and left wrists. The patch antenna is fabricated on a RT/Duroid board of dielectric constant $\epsilon_r = 3$ and thickness 1.524 mm and has a total board size of 60×65 mm^2 ($0.49\lambda \times 0.53\lambda$ at 2.45 GHz) and patch size of 34.95×39.5 mm^2. Table I presents the main antenna parameters when placed in free space and on the body.

The on-body antenna performance is numerically investigated (in addition to experimentally) by applying a one-layer human tissue slab model (muscle with $\epsilon_r = 52.8$ and conductivity of 1.7 S/m at 2.4 GHz, dimensions: $120 \times 120 \times 40$ mm^3) using finite element method utilized in HFSS. The detuning experienced when placed on the body is not significant due to the ground plane size, however, for smaller antennas and ground planes the detuning will be more significant [14], [15]. The antenna used here was chosen as a reference to mainly emphasize on radio channel behavior. The antenna is a major part of any communication system and its effect is quite often not separable from
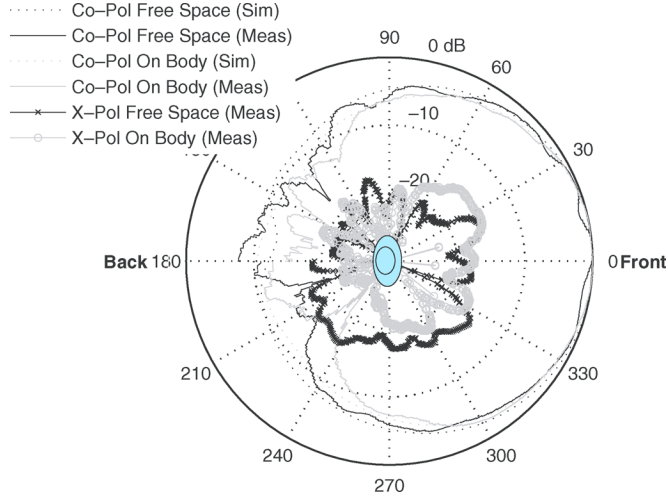
Fig. 1. Radiation patterns at the azimuth plane of the antenna when placed in free space and on the chest with the radiating patch facing outwards and antenna placed parallel to the body.

TABLE II
FIRST ORDER STATISTICS FOR VARIOUS BODY ACTIVITIES AND POSTURES BASED ON CHAMBER MEASUREMENT (ALL VALUES ARE IN DECIBELS)

Rx		Chest	Back	Head Left	Head Right	Wrist Left	Wrist Right
Standing	μ	42.0	58.8	49.8	56.9	50.5	65.5
	δ	1.9	4.3	4.8	5.4	6.2	7.9
Sitting	μ	36.6	68.7	47.3	57.0	49.4	64.5
	δ	0.6	3.3	0.8	1.6	9.7	10.0
Static	μ	41.2	60.2	49.4	56.9	50.3	65.3
	δ	2.6	5.4	4.5	5.0	6.7	8.2
Dynamic	μ	41.1	60.1	48.2	52.9	46.3	62.0
	δ	3.6	5.1	4.3	6.9	8.8	9.3

the propagation channel [7]–[9], [18]. Radiation performance of the antenna when placed on the trunk of the body was experimentally measured and compared to the pattern obtained in free space and also to simulated patterns obtained by numerical modelling techniques, Fig. 1.

B. Statistical Analysis of On-Body Propagation

On-body propagation links can be roughly categorized according to the parts of the body to which both transmit and receive antennas are attached, e.g., trunk-to-trunk, trunk-to-head and trunk-to-hand [6], [9], [11]. A trunk-to-limb link is expected to be subject to significant variation due to the movement of the limb while a trunk-to-trunk link will be more stable. The main difference between receivers positioned on the chest and the back (with respect to transmitter on the left side of the waist) is that the latter link is shadowed by the trunk and it is verified from the measurement results with extra attenuation of 19.2 dB in the back position. The mean attenuation due to different head movements (e.g., head turning left and right) is approximately 13 dB.

A comparison between body activities such as 'Standing' and 'Sitting' is demonstrated in Table II based on data collected in the chamber, when the movements have reached a steady state for each relevant body posture. When sitting, a decrease in attenuation of 5.4 dB on the chest is obtained and an increase in attenuation on the back by 9.9 dB is also deduced. For the other receiver positions, the difference in mean attenuation between "standing" and "sitting" is smaller because the position of these receivers with respect to the transmitting antenna remains unaffected.
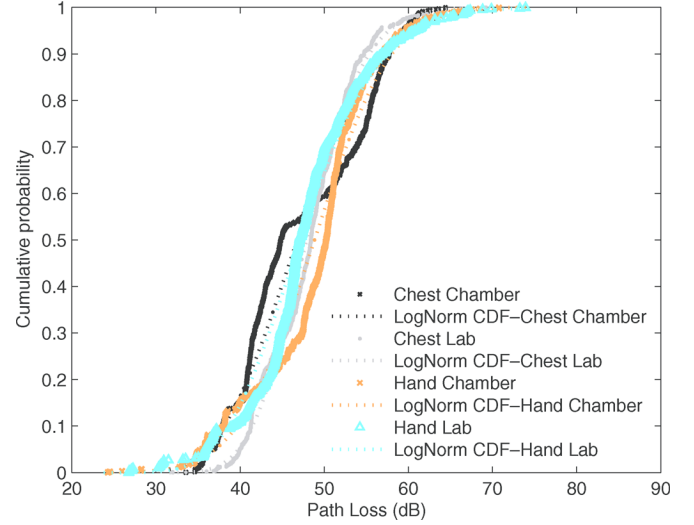

Fig. 2. Measured CDF of path loss data for specific on-body scenarios including both co-pol and cross-pol data in the chamber and the lab fitted to lognormal distribution, trunk to chest (Rx1, Fig. 1) radio link in the chamber and the lab and trunk to hand (Rx5, Fig. 1) radio link in the chamber and the lab with data fairly fitting lognormal distribution.

The measured data is statistically analyzed by means of fitting to well-known empirical distributions. The lognormal cumulative distribution function (CDF) is commonly used for communication oriented radio channel analysis and often described by μ and σ representing the (log) location and the (log) scaling factor of the data [16]. The CDF of the measured path losses for trunk to chest and trunk to hand (left wrist) scenarios in the chamber and lab is calculated respectively and presented in Fig. 2. CDF of measured data fits well to lognormal distribution (chamber: $\mu = 3.85$, $\sigma = 0.16$ and lab: $\mu = 3.86$, $\sigma = 0.11$) which depends on the generation of a random variable. However, in the case of receiving antenna placed on the chest and measured in the chamber, the distribution deviates at a greater rate from the modelled lognormal fit. This is due to the mismatch of antenna polarization during body movements and position changes and non-reflecting environment in the chamber. In the trunk to hand case, measured data from both chamber and lab fits well to lognormal distribution (chamber: $\mu = 3.85$, $\sigma = 0.15$ and lab: $\mu = 3.84$, $\sigma = 0.16$), which can be explained by referring to measured path loss variation presented in [6], [9], which illustrates the similarity in both co-polarization and cross-polarization data. Regarding the modelled distribution parameters, the scaling factor σ is quite similar in most cases presented in Fig. 2. In the case when receiver is placed on the chest, σ becomes smaller ($\sigma = 0.11$, representing narrower spread of data), which demonstrates stability of the channel and multipath contribution in the dense indoor environment.

The measured path loss data including all body postures is modelled by obtaining its probability distribution functions (PDF) in the chamber and the lab, Fig. 3(a). The PDF fits to lognormal Gaussian distribution (chamber: $\mu = 3.93$, $\sigma = 0.23$ and lab: $\mu = 3.87$, $\sigma = 0.24$). In addition, an important factor to account for when modelling radio channels is shadowing factor, which can be quantified by calculating the deviation of path losses. Fig. 3(b) shows the CDF of deviation in the chamber and lab with corresponding normal distribution ($\sigma = 12.38$). In both cases, path loss deviation can be predicted by fitting to the same normal distribution independent of environment. This indicates that human body shadowing is the main factor of path loss variation in on-body radio channels.
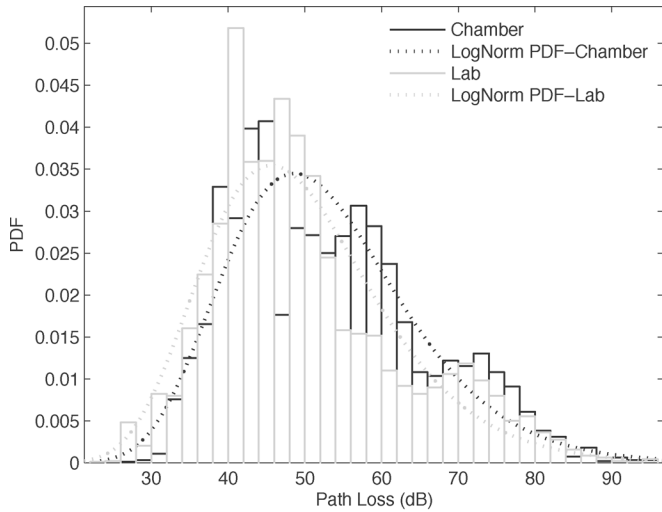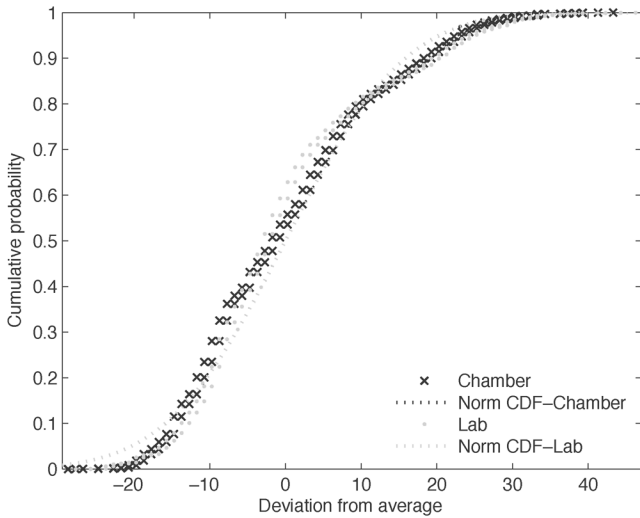
Fig. 3. (a) PDF of measured path loss in all scenarios (Rx1–Rx6, Fig. 1) in the chamber and the lab including channel data for all investigated on-body links and body movements fitted to a Gaussian distribution and (b) CDF of measured deviation from average received power calculated from total measurement data which fits a normal distribution very well (represent shadowing).

The effects of different antenna types such as monopole, dipole and patch array on the radio channels for on-body communication for both narrowband and ultrawideband propagation have been investigated and analyzed in [6], [9] and [14]. Results proved that monopole antennas provided best performance for various on-body links, however, microstrip antennas still present a favorable choice due to ease of fabrication, cost-effectiveness and potentially being conformal to the body. Antenna orientation and polarization influence is also analyzed and it was demonstrated that receiving different polarization simultaneously would improve communication links, therefore dual-polarized antenna would provide suitable solution for wireless body area network (BAN) applications.

III. RADIO SYSTEM MODELLING AND ANALYSIS

A. System-Level Modelling

Applying Gaussian frequency shift keying (GFSK) modulation and transmission techniques utilized in Bluetooth technology [16], [17], system-level modelling of suitable transmitter and receiver architecture is performed for data rates up to 1 Mbit/s in raw data and voice communication modes based on GFSK modulation and decoding procedures.

TABLE III
PERCENTAGE OF TIME BER $<0.1\%$ (TX ON THE LEFT SIDE OF THE WAIST)

Transmit Power	Chest	Back	Head		Hand	
			Left	Right	Left	Right
-20 dBm	>99	98.5	99	>99	99	96
-30 dBm	>99	81.6	>99	98.5	88.6	64
-40 dBm	72	11.7	98	86	45.3	10.3

The radio system model was based on typical Bluetooth transceiver with channel parameters derived in the previous section incorporated within the communication link.

Bluetooth applies GFSK modulation with nominal modulation index $h_f = 0.33$ and $B_b T = 0.5$, which presents the normalized bandwidth of the pre-modulation Gaussian low pass filter where B_b is the 3 dB bandwidth and T is the bit period. The steps for GFSK signal generation and Bluetooth symbol control are defined in [17].

B. System Performance Analysis

As a measure of performance the bit error rate (BER) of the system is calculated with regards to sensitivity level and the effect of signal to noise ratio (SNR) on system performance. Measured channel data (in lab) used for system performance evaluation include direct paths, multipath components and channel noise and their variation due to body postures and movements. BER performance of GFSK depends on the channel and system applied, either coherent or noncoherent. In coherent non-fading environment, the probability of error in the higher bound of SNR can be approximated as [17], [19]

$$P_e \left(\frac{E_b}{N_0} \right) \cong \frac{1}{2} erfc \left(\alpha \frac{E_b}{N_0} \right) \tag{1}$$

where E_b/N_0 is the received signal energy-to-noise density ratio and α is a constant parameter that approximately equals to 0.68 for GFSK with $B_b T = 0.25$ and 0.85 for simple minimum shift keying modulation as $B_b T \to \infty$ [19]. On the other hand, if the environment experiences fast and deep multipath fading caused by moving receiver which is usually modelled by Rayleigh fading, the BER performance ban be estimated as [19],

$$P_e(\Gamma) \cong \frac{1}{4\alpha\Gamma} \tag{2}$$

where Γ is the average E_b/N_0. Those assumptions are applied in order to study the BER performance of a GFSK radio system with channel parameters obtained from measured data in order to highlight on-body radio propagation effects on a standard commonly used narrowband system.

The BER performance is calculated against different transmit power levels for specific SNR. In both scenarios (trunk-to-hand and trunk-to-head), excellent system performance achieved for transmit power down to 0.01 mW, and acceptable performance was obtained for values down to 0.001 mW. For lower transmit powers ($< 100 \, \mu W$), higher bit error rates resulted in degrading the overall system performance (Table III). The percentage of time when the bit error rate is less than 0.1% (Bluetooth, short-range wireless communication) is presented in Table II; outage rates are low for powers down to -30 dBm. The calculated BER for different on-body scenarios and for low transmit power is presented in Fig. 4. As expected trunk-to-back has the worst performance due to dominant non line-of-sight (NLOS) communication, while when the receiver is placed on the chest, better BER performance is achieved.

The analysis above is also performed for lower data rates to examine the BER outage rate against time for various values for low-rate applications. The BER performance is improved when the data rate is decreased for a specific on-body scenario with transmit power set to
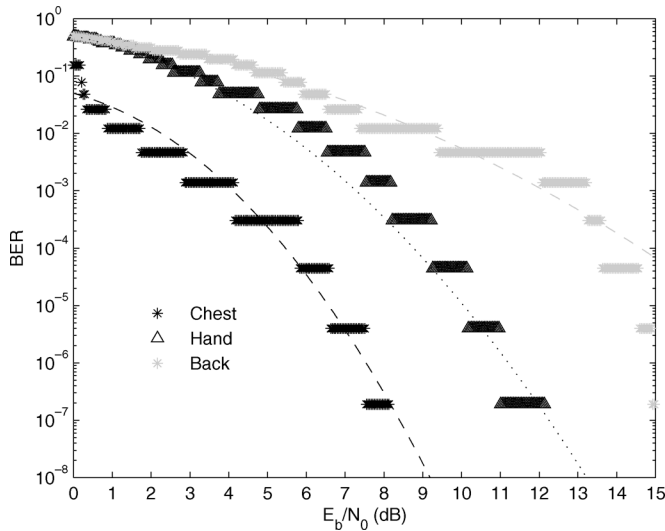
Fig. 4.   BER versus bit energy-to-noise density for different on-body scenarios (Rx on chest, left wrist and back). Dotted lines present best fit for the calculated BER.
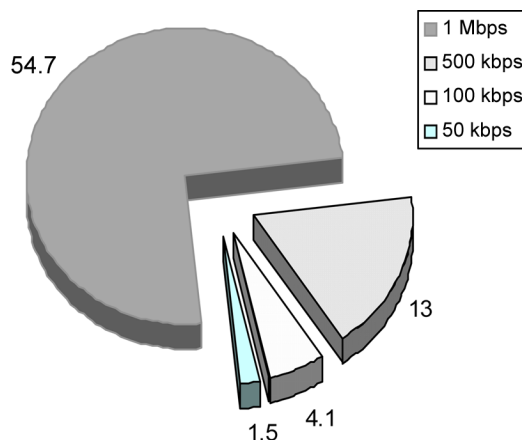

Fig. 5.   Pie chart presenting the percentage of time BER is greater than 0.1% (scenario trunk-to-left hand with transmit power of −40 dBm, Rx5, Fig. 1).

−40 dBm, as generally expected for any radio system. This leads to changes in BER performance as a function of time for the on-body radio links. The percentage of time the BER value is greater than $1e-3$ (Outage rate) is 54.7%, 13%, 4.1% and 1.5% for 1 Mbps, 500, 100, and 50 kHz, respectively, for trunk-to-left wrist scenario, which proves performance enhancement for lower data rate applications with low transmit power, Fig. 5.

IV. CONCLUSION

On-body propagation measurement using microstrip patch antennas at 2.45 GHz in an anechoic chamber and in the lab has been presented. The measurements were taken for a range of body positions and postures, thereby allowing a subsequent investigation in the effects of body motion on the received signal. The results demonstrated that attenuation caused by trunk, head and jumper is around 19.2, 13.0, and 1.7 dB, respectively. Statistical channel models and parameters were derived for on-body channels with respect to different links and body scenarios and also compared to empirical wireless propagation models for cross

referencing and evaluation. A system model based on the GFSK modulation scheme utilized in Bluetooth specifications was performed. Excellent bit error rate is achievable for transmitting powers down to 0.01 mW. The dependency of system performance on the applied data rate was also demonstrated and it was shown that acceptable BER can be achieved for power levels as low as −40 dBm for low data rates commonly used in health monitoring applications and general wireless sensor networks.

REFERENCES

[1] J. Bernardhard, P. Nagel, J. Hupp, W. Strauss, and T. von der Grun, "BAN-body area network for wearable computing," presented at the 9th Wireless World Research Forum Meeting, Zurich, Jul. 2003.

[2] E. Jovanov, A. O'Donnell-Lords, D. Raskovic, P. Cox, R. Adhami, and F. Andrasik, "Stress monitoring using a distributed wireless intelligent sensor system," *IEEE Eng. Medicine Biology Mag.*, vol. 22, no. 3, pp. 49–55, May/Jun. 2003.

[3] C. Kunze, U. Grossmann, W. Stork, and K. Muller-Glaser, "Application of ubiquitous computing in personal health monitoring systems," in *Biomedizinische Technik: 36th Annual Meeting of the German Society for Biomedical Engineering*, 2002, pp. 360–362.

[4] N. F. Timmons and W. G. Scanlon, "Analysis of the performance of IEEE 802.15.4 for medical sensor body area networking," in *1st Annual IEEE Communications Society Conf. Sensor and Ad Hoc Communications and Networks (SECON)*, Oct. 4–7, 2004, pp. 16–24.

[5] Internet resource, Ubiquitous Communication Through Natural Human Actions [Online]. Available: http://www.redtacton.com/en/

[6] Y. Nechayev, P. Hall, C. C. Constantinou, Y. Hao, A. Owadally, and C. G. Parini, "Path loss measurements of on-body propagation channels," in *Proc. Int. Symp. Antennas and Propagation*, Sendai, Japan, Aug. 2004, pp. 745–748.

[7] A. Alomainy, Y. Hao, C. G. Parini, and P. S. Hall, "Comparison between two different antennas for UWB on-body propagation measurements," *IEEE Antennas Wireless Propag. Lett.*, vol. 4, no. 1, pp. 31–34, Dec. 2005.

[8] A. Alomainy, Y. Hao, X. Hu, C. G. Parini, and P. S. Hall, "UWB on-body radio propagation and system modelling for wireless body-centric networks," *Proc. Inst. Elect. Eng. Communications-Special Issue on Ultra Wideband Systems, Technologies and Applications*, vol. 153, no. 1, Feb. 2006.

[9] P. S. Hall, Y. Nechayev, Y. Hao, A. Alomainy, M. R. Kamarudin, C. C. Constantinou, R. Dubrovka, and C. G. Parini, "Radio channel characterisation and antennas for on-body communications," in *Proc. Loughborough Antennas and Propagation Conf.*, Loughborough, U.K., Apr. 2005, pp. 330–333.

[10] P. Hall, M. Ricci, and T. Hee, "Characterization of on-body communication channels," in *Proc. 3rd Int. Conf. Microwave and Millimeter Wave Technology*, Beijing, China, Aug. 2002, pp. 770–772.

[11] Y. Hao, A. Alomainy, P. S. Hall, Y. I. Nechayev, C. G. Parini, and C. C. Constantinou, "Antennas and propagation for body centric wireless communications," presented at the IEEE/ACES Int. Conf. Wireless Communications and Applied Computational Electromagnetics, Honolulu, HI, Apr. 3–7, 2005.

[12] T. Zasowski, F. Althaus, M. Stager, A. Wittneben, and G. Troster, "UWB for noninvasive wireless body area networks: channel measurements and results," in *Proc. IEEE Conf. Ultra Wideband Systems and Technologies*, Reston, VA, Nov. 2003, pp. 285–289.

[13] P. D. Gift, D. K. Choudhury, D. N. Cassadine, S. M. Yano, T. B. Welch, R. L. Musselman, and B. A. Emessiene, "The effects of the human body on UWB signal propagation in an indoor environment," *IEEE J. Select. Areas Commun.*, vol. 20, no. 9, pp. 1778–1782, Dec. 2002.

[14] M. R. Kamarudin, Y. I. Nechayev, and P. S. Hall, "Performance of antennas in the on-body environment," in *IEEE Antennas and Propagation Society Int. Symp.*, Washington DC, Jul. 3–8, 2005, vol. 3A, pp. 475–478.

[15] M. Klemm, I. Z. Kovcs, G. F. Pedersen, and G. Troster, "Novel small-size directional antenna for UWB WBAN/WPAN applications," *IEEE Trans. Antennas Propag.*, vol. 53, no. 12, pp. 3884–3896, Dec. 2005.

[16] R. Steele and L. Hanzo, *Mobile Radio Communications*, 2nd ed.   New York: Wiley, 1999.

[17] Bluetooth Specifications vol. 2, Nov. 2003 [Online]. Available: http://www.bluetooth.org

[18] R. Vaughan and J. B. Andersen, *Channels, Propagation and Antennas for Mobile Communications, Electromagnetic Waves Series 50*. London, U.K.: Institute of Electrical Engineers (IEE), 2003.

[19] K. Murota and K. Hirade, "GMSK modulation for digital mobile radio telephony," *IEEE Trans. Commun.*, vol. COM-29, no. 7, pp. 1044–1050, Jul. 1981.